A Screening Process for Carbonation of Vegetable Oils Using an Aluminum(salen) Complex with a Further Application as Weldable Polymers

Rafael T. Alarcon, Katie J. Lamb, Éder T.G. Cavalheiro, Michael North, Gilbert Bannach**

R.T. Alarcon, E.T.G. Cavalheiro - University of São Paulo, São Carlos Institute of Chemistry, São Carlos, São Paulo 13566-590, Brazil
K.J. Lamb - University of Sheffield, Department of Chemical and Biological Engineering, Mappin Street, Sheffield, S1 3JD, United Kingdom.
M. North - The University of York, Green Chemistry Centre of Excellence, Department of Chemistry, Heslington, York, YO10 5DD, United Kingdom.
R.T. Alarcon, G. Bannach - UNESP - São Paulo State University, School of Science, Department of Chemistry, Bauru, São Paulo, 17033-260, Brazil.

*Corresponding author. E-mail: gilbert.bannach@unesp.br; michael.north@york.ac.uk

Keywords: *Cyclic carbonate; renewable material; weldable material; Brazilian biomass; Greenhouse utilization; aluminum catalyst.*

ABSTRACT

Carbon dioxide (CO_2) occurs naturally, though its emissions have been increasing due to anthropogenic activities, and its increasing atmospheric concentration levels are causing a greenhouse effect. In efforts to develop new carbon dioxide utilization (CDU) methodologies, the catalyzed reaction of CO_2 with epoxidized vegetable oil, obtained from Brazilian Macaw oil and Baru oil, to form carbonated oils for novel and sustainable monomers was explored. A screening process is carried out to develop the best reaction conditions, by varying catalyst/co-catalyst loading, reaction time, CO_2 pressure, and the reaction temperature, resulting in conversions of 100%. The aluminum(salen) complex shows a selective and efficient catalyst activity. Both carbonated oils are reacted with amines (1,6-diaminohexane, lysine, and 4,4'-methylenebis(cyclohexylamine)) to provide weldable polyhydroxyurethanes. Polymers synthesized from lysine provide a more selective reaction and higher cross-linked structures, with fewer side reactions involving the glyceride groups. All the synthesized polymers are thermally stable above 200 °C and DSC analysis shows two main thermal events, related to the glass transition (T_g) and the topology-freezing transition temperature (T_v). The T_v result indicates that the polymer has weldable properties due to chemical bond exchange. Thus, these polymers can be healed into different shapes upon exposure to red light (660 nm).

INTRODUCTION

Carbon dioxide (CO_2) is the main cause of the greenhouse effect and its abundance has increased over recent years due to anthropogenic activities. Anthropogenic activity is responsible for 33% of all CO_2 in the atmosphere, which is increasing by 37,000 megatons per year.[1,2] Therefore, a need for CO_2 utilization has emerged to reduce these emissions. Carbon dioxide can be used as a reactant to produce new chemicals and materials; however, it is not reactive at room temperature and at atmospheric pressure, so high temperatures and/or pressures, with the use of catalysts, are necessary.[3,4] Carbon dioxide has a positive charge by polarization at the central carbon atom and can react with epoxides (which act as a nucleophile) to provide cyclic carbonates.[4] This cycloaddition reaction is sustainable and presents an atom efficiency of 100% (i.e. all reactants are embodied in the final product). This process generally does not require solvents and is thermodynamically favorable.[2,5]

Cyclic carbonates have been widely synthesized from renewable feedstocks to produce polymeric materials.[6] Amongst the most versatile chemicals are unsaturated vegetable oils (triacylglycerols) which can form multi-carbonate structures. Carbonated vegetable oils are sustainable monomers and are used to produce cross-linkable polymers.[7] The most commonly used cross-linkers are amines, which provide polyhydroxyurethanes. These polymers are greener than conventional polyurethanes, which are made from isocyanates. The polyurethane market is large and had an estimated value of 7 billion USD in 2019.[7] Polyhydroxyurethanes from vegetable oils are sustainable materials and can be classified as biomass-derived polymers. Therefore, they can act as substitutes for petrochemically derived polymers. The use of biomass-derived polymers worldwide is increasing annually, with 7.59 million tonnes of biomass-derived polymer predicted to be produced by 2026.[7,8]

Although fundamental in the global food chain, soybean oil is usually used as the precursor to carbonated monomers due to its ease of acquisition. In this study, we synthesized carbonated vegetable oils from Brazilian biomass, in particular Baru oil and Macaw oil, which are excellent alternatives to soybean.[9]

The carbonation reaction was assisted by an aluminum(salen) complex that is both a selective and highly efficient catalyst. The catalyst was designed to be soluble in organic media and greener as aluminium is the most abundant metal in the Earth's crust and its industrial production is well-known.[12] Salen compounds have shown great potential as catalysts for carbonatation processes, especially when coordinated with metals in the 3+

oxidation state such as cobalt, chromium and aluminum.[1,11] The salen ligand with *tert*-butyl and cyclohexyl groups was selected to enhance the solubility of the complex in highly non-polar triglyceride derivatives.[10,11] Furthermore, this bimetallic aluminium(salen) complex has exhibited excellent activity for internal epoxide groups, though this is its first test with vegetable oils.[11]

After a reaction parameter screening process, 100% conversion was obtained for both Baru and Macaw vegetable oil. Polymers were then consequently synthesized with the carbonates formed using three different amines, all of which presented self-healing properties using LEDs with a red emission (660 nm).

MATERIALS AND METHODS

Materials

Macaw vegetable oil (MWO, leaking data: 03/2019; batch code: MAO073/18) and Baru vegetable oil (BO, batch code: MAO073/18; leaking data: 03/2019) were acquired from Mundo dos Óleos (Brasília, Brazil). Amberlite IR120, hydrogen peroxide (30% H_2O_2), glacial acetic acid (≥ 99%), tetraethylammonium bromide (TEAB; 99%), tetrabutylammonium bromide (TBABr; ≥ 99%) perchloric acid (70%), ethyl acetate (99.8%), acrylonitrile (≥ 99%), (*R,R*)-(−)-*N,N′*-bis(3,5-di-tert-butylsalicylidene)-1,2-cyclohexanediamine (98%), and aluminum ethoxide (97%) were acquired from Sigma-Aldrich and utilized without further pre-treatment or purification The iodine value for MWO and BO was calculated in triplicate using the Wijs method, following the standard ASTM D5554-15 method,[13] resulting in 103.5 ± 0.9 g of I_2 per 100 g for BO (0.408 ± 0.003 mol of alkenes per 100 g) and 116.0 ± 0.6 g of I_2 per 100 g for MWO (0.457 ± 0.002 mol of alkenes per 100 g). The average number of double bonds per molecule of BO and MWO is equal to 3.5 and 4.0, respectively. Hence, it is possible that the main structures utilized in BO are a triacylglycerol with 3 oleic acid groups, (i.e. C18:1, with a total of 3 double bonds) and a triacylglycerol with 2 oleic and 1 linoleic acid group (i.e. C18:2 with a total of 4 double bonds). It was therefore possible to calculate that the average molecular mass of the BO used as 885.4321 Da. The main structure of the MWO can be two linoleic acids and one palmitic acid (i.e. C16:0) or a structure with one linoleic acid and 2 oleic acids. Thus, the average molecular mass of MWO is estimated to be 855.3603 Da.

Syntheses of epoxidized and carbonated baru and macaw vegetable oils

The epoxidation of MWO and BO were performed according to the literature procedure,[14] resulting in an epoxidized macaw oil (EMWO) with 0.434 ± 0.006 mol of oxygen in an epoxide environment and epoxidized baru oil (EBO) with 0.406 ± 0.003 mol of oxygen in epoxide environments (as determined by performing the standard ASTM D1652-11 titration method in triplicate).[15] Hence, the conversion of alkenes into epoxide was 95% for EMWO and ≈ 100% for EBO.

For the carbonation reaction, a screening process was carried out to identify the optimal catalyst amount, time, CO_2 pressure, and temperature. Firstly, 0.1 mmol of EBO with average molecular weight equal to 933.4303 Da or EMWO with average molecular weight equal to 915.3289 Da were added to a glass vial along with different amounts (mol% with respect to the epoxide) of aluminum(salen) complex (AlSC), tetraethylammonium bromide (TBABr) and a magnetic stirrer bar. Thereafter, the vial was placed into a high-pressure Parr reactor and charged with CO_2 gas (99.9%). The reactor was heated using an aluminum base plate and jacket, and was kept at the desired temperature for the desired time whilst stirred. Thereafter, the crude product, with a conversion of 100% (Carbonated Baru oil - CBO) was purified and analysed was purified and analysed by ESI-Mass Spectrometry. Firstly, ethyl acetate (20 mL) was added to cause the AlSC to precipitate, then the solution was filtered to give a reddish high-viscous liquid. Secondly, the solution was washed with hot water (30 mL) three times to remove the TBABr. Finally, the solution was dried with magnesium sulphate ($MgSO_4$) and evaporated *in vacuo* to give an orange highly-viscous liquid (as shown by Figure S1 in the Supporting Information). In addition, the carbonated baru oil (CBO) and carbonated macaw oil (CMWO) were analysed by ^{1}H-NMR and MIR spectroscopy without purification. The best experimental conditions (which achieved 100% conversion) was then used to perform a scaled-up reaction, to producing 30.0 g of CBO and CMWO, which were used further in the polymerization reactions.

The aluminum(salen) complex (AlSC) was synthesized following the standard literature procedure, without any experimental modifications.[11] The ^{1}H-NMR spectrum for AlSC and the signals descriptions are found in the Supporting Information (Figure S2).

Polymerization reaction

For the polymerization reaction, three diamines were selected as cross-linkers: 1,6-diaminohexane (HDA), lysine (LYS), and 4,4'-methylenebis(cyclohexylamine)

(MBCA). Firstly, CBO or CMWO was poured into a beaker containing a cross-linker in equimolar quantity, considering the number of carbonate and amine groups. The mixture was then heated at 50 °C and stirred for 1 hour to form a prepolymer. Thereafter, the prepolymer was added to a silicon tray and cured at 140 °C for several hours. The reaction was monitored over time (12 h) by mid-infrared spectroscopy (MIR) to determine the best polymerization time. The final polymers were termed CBO-HDA, CBO-LYS, CBO-MBCA, CMWO-HDA, CMWO-LYS and CMWO-MBCA, depending on the cross-linkers and carbonated oils used. All polymers underwent thermal characterizations and gel content determination. The complete scheme for epoxidation, carbonation and polymerization, showing the catalyst and cross-linkers used is shown in Figure 1.

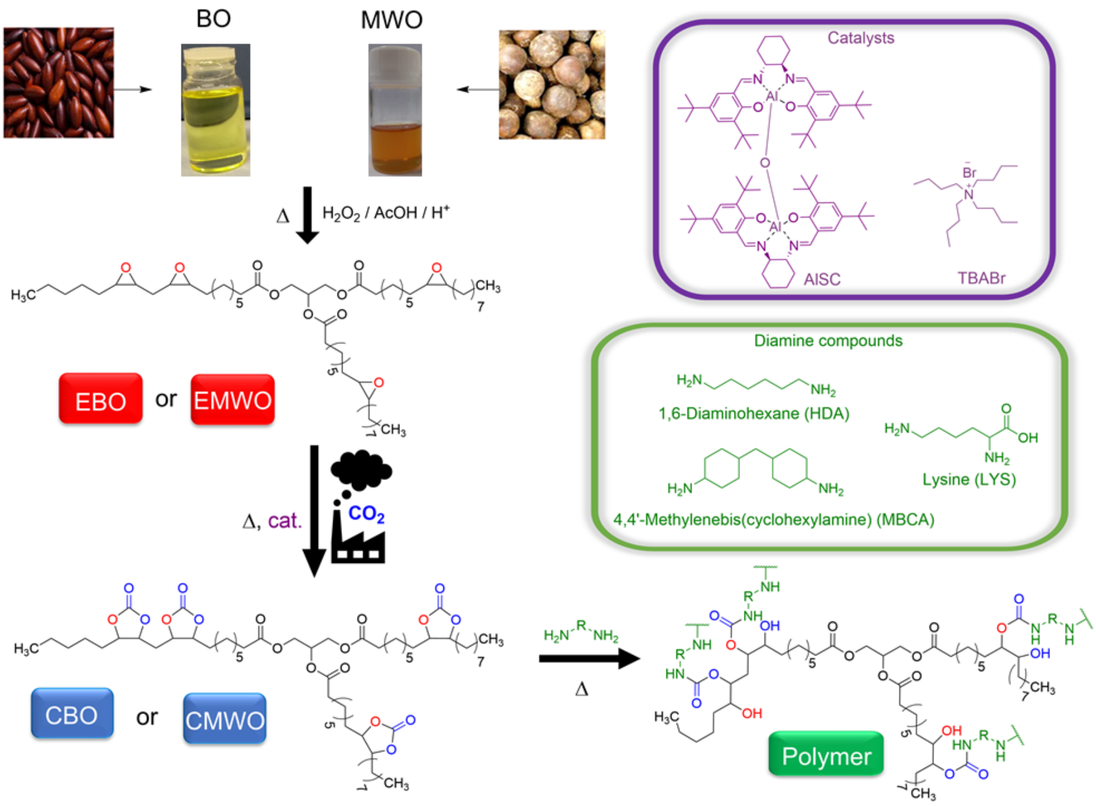

Figure 1. Reactions steps, cross-linkers, and catalysts employed in this study.

Mid-infrared spectroscopic analysis (MIR)

MIR spectra for EMWO, EBO, CMWO, and CBO and polymers were obtained using a Bruker Vertex 70 FT-IR spectrometer, with attenuated total reflectance (ATR) using a diamond crystal, in the region of 4000-500 cm^{-1} (with a resolution of 4 cm^{-1}). The carbonate group consumption during the polymerization reaction was calculated by Equation 1. Hence, the conversion of carbonate (CC) groups into urethane groups was determined. The term $(A_{C=O}/A_{C\text{-}H})_0$ is the absorbance area for the carbonate stretching peak (1803 cm^{-1}), at time = 0 seconds, normalized by the area of the C-H stretching IR band (2952 cm^{-1}), while the term $(A_{C=O}/A_{C\text{-}H})_t$ was acquired over time (every 24 h).

$$CC\ (\%) = \left[1 - \frac{(\frac{A_{C=O}}{A_{C-H}})_t}{(\frac{A_{C=O}}{A_{C-H}})_0}\right] \qquad \text{(Equation 1)}$$

^{1}H-NMR analysis

To determine the principal signals of EBO, EMWO, and the synthesized carbonated oils, ^{1}H-NMR spectroscopy was performed, using a Jeol 400 MHz spectrometer. Samples were dissolved in deuterated chloroform ($CDCl_3$, 99.8% D, Sigma-Aldrich). The AlSC catalyst was also analysed using the same equipment and NMR solvent.

ESI Mass Spectrometry

Mass spectra were recorded on a Bruker compact time-of-flight mass spectrometer (microTOF) MS, twinned with an Agilent series 1260 LC for Electrospray Ionisation (ESI) and Atmospheric Pressure Chemical Ionisation (APCI) analysis. Samples were dissolved in CH_2Cl_2 prior to analysis.

Thermal analysis: simultaneous thermogravimetry-differential thermal analysis (TG-DTA), differential scanning calorimetry (DSC) and dynamic mechanical analysis (DMA)

Simultaneous TG-DTA curves for all polymers were obtained using a Netzsch STA 449 F3 simultaneous module. Samples (30 mg) were placed into an α-alumina open crucible (200 μL), and curves were obtained at a temperature range of 30 °C to 650 °C, applying a heating rate of 10.0 °C min^{-1} with a flow rate of 70.0 mL min^{-1} under a dry air atmosphere.

DSC analyses were performed in a TA Instruments DSC apparatus (model DSC-Q10 modulus) using 10 mg of sample, which were analyzed in a 40-μL closed aluminum crucible with a perforated lid. The samples, were heated from -35 °C to 150 °C, with a dynamic N_2 atmosphere (50.0 mL min^{-1}) and a heating rate of 10.0 °C min^{-1}.

DMA analyses were executed in a Q800 apparatus (TA instruments). The polymer samples were cut into pieces of 20 mm length, 5 mm width and 1 mm thickness prior to analysis and analyzed from -50 °C to 100 °C under a N_2 atmosphere, using a frequency of 1 Hz and a heating rate of 3 °C min^{-1}. The DMA provided curves which were used to obtain storage modulus (E') and $tan\text{-}\delta$ values. The cross-link density (v) was determined by Equation 2. *E'* is the storage modulus (rubbery region), *R* is the gas constant (8.314 J K^{-1} mol^{-1}), and *T* (K) is the rubbery temperature ($tan\text{-}\delta$ + 40 °C).

$$v = E'/3RT \qquad \text{(Equation 2)}$$

The tensile test (stress x strain curves) for each polymer was determined in the same DMA equipment at 30 °C.

Gel Content

The gel content (GC) was determined according to the literature method.[17] Each polymer was weighted (Initial weight - W_i) and added to a paper cartridge, which was then placed in a Soxhlet apparatus. The cartridge was then refluxed with ethyl acetate for 8 h. Thereafter, the polymer was dried in an oven at 80 °C for 3 h and weighed again (to obtain the final weight - W_f). Gel content value is determined by Equation 3.

$$GC\ (\%) = \left(\frac{w_f}{w_i}\right) \times 100 \qquad \text{(Equation 3)}$$

Polymer reprocessing

The polymer sample was first chopped into square pieces and added into a circular Teflon® matrix. Thereafter, pieces were heated by a red LED lamp (PR160L, 660 nm, 40 w) from Kessil for 2 min with pressure (50 Bar) applied onto the heated polymer. After the remolding process, the polymer was cooled to room temperature.

RESULTS AND DISCUSSION

Screening process for the carbonation reaction

Different temperatures, pressures and catalyst amounts were used in these reactions. Firstly, EBO was used in the carbonation reaction as shown in Table 1. The first reaction was performed at 60 °C and a pressure of 10 bar using only AlSC (2.5 mol%). After 24 h, no conversion was observed. Thereafter, a reaction using only TBABr was performed using the same reaction temperature, pressure and time, with only a small conversion observed (5%). The third reaction used the same conditions with both AlSC and TBABr present (in the same proportions). Consequently, the conversion increased to 28%. This result proves that there is a synergic effect between AlSC (the reaction catalyst) and TBABr (the reaction co-catalyst). The next reaction was performed at 60 °C using 5.0 mol% of AlSC and TBABr. Consequently, the conversion reached 63% (CBO-2), which was twice as high as the previous reaction conditions. Thereafter, the temperature was increased to 80 °C and used 2.5 mol% of both catalysts was used with 10 bar of CO_2 pressure. This reaction obtained a conversion of 59% (CBO-3), which was close to the result for CBO-2. Thereafter, two reactions were performed using 2.5 mol% of AlSC and 5 mol% of TBABr (CBO-4) and then 5.0 mol% of AlSC and 2.5 mol% of TBABr (CBO-5), which resulted in conversions of 85% and 58%, respectively. Despite the increase in the amount of AlSC used during reaction CBO-5, a similar conversion to CBO-3 (59%) was obtained. This result showed that greater amounts of AlSC do not assist the carbonation reaction. On the other hand, the increase in amount of TBABr improved the conversion. The AlSC catalyst acts as a Lewis acid (LA) and acts exclusively in epoxide ring activation reactions, but it does not cleave the epoxide ring. On the other hand, TBABr acts directly in the cleavage process, due to halide (Br^-), and counterion [Bu_4N^+], formation. Thus, greater amounts of TBABr increases carbonation conversion, while AlSC does not. The catalytic reaction mechanism can be seen in Figure S3 in the Supporting Information. To prove that both catalysts were necessary, a new control reaction was performed using only 5.0 mol% of TBABr (CBO-6), which resulted in a conversion of 26%.

At this point, it was determined that 5.0 mol% TBABr should be used in all further reactions. To further increase the conversions obtained, the temperature reaction was increased to 100 °C, whilst maintaining a CO_2 pressure of 10 bar. A reaction was also performed in which the temperature was held at 80 °C and the pressure was increased to 15 bar. The reaction at 100 °C used 2.5 mol% of AlSC (CBO-7) and 5.0 mol% of TBABr after 24 h reached a conversion of 100%. Thereafter, a new reaction was performed using 1.2 mol% of AlSC to also provide a conversion of 100% (CBO-8). This result showed that only a small quantity of AlSC is necessary to active the epoxide ring. The reactions performed at a temperature of 80 °C, a CO_2 pressure of 15 bar and 5.0 mol% of TBABr exhibited conversions of 90% (CBO-9) and 94% (CBO-10), using 2.5 mol% and 1.2 mol% of AlSC, respectively. These results highlighted that increasing the pressure does increases the conversions to nearly 100%, but the conversions could be increased more sufficiently by increasing the reaction temperature. Reaction CBO-11 (where the temperature was 100 °C) gave a conversion of 65% using 2.5 mol% of TBABr. This again highlighted the importance of using 5.0 mol% of TBABr in the reaction process.

In order to further reduce the AlSC loading, new reactions were carried out at 100 °C and using 5.0 mol% of TBABr at a CO_2 pressure of 10 bar. A conversion of 98% was obtained with only 0.6 mol% of AlSC (CBO-12), which was a good result. Reducing the amount of AlSC decreased the obtained carbonation conversions, due a less effective epoxide ring activation process. Consequently, some parameters were fixed at this point for the EBO carbonation reaction (temperature = 100 °C; pressure = 10 bar of CO_2; AlSC = 1.2 mol%; and TBABr = 5.0 mol%). Further screening reactions were then performed to reduce the reaction time. The first two reactions performed (CBO-13 and CBO-14) showed lower conversions of 56% (AlSC= 2.5 mol% and TBABr = 5.0 mol%) and 61% (AlSC = 1.2 mol% and TBABr = 5.0 mol%) after 6 h, respectively. When the time was increased to 12 h, this was not enough to convert 100% of the epoxide rings into five membered-carbonated rings (reactions CBO-15 and CBO-16). All of the screening experiments performed are shown in Table 1. As a result, it is possible to consider CBO-8 as the best experimental conditions, as this reaction achieved the highest conversions in the shortest time and using only 1.2 mol% of AlSC.

Table 1. Conversion of EBO and EMWO oil into cyclic carbonate.

Sample	*AlSC (mol%)	*TBABr (mol%)	Temperature (°C)	Pressure (Bar)	Time (h)	Conversion (%)
CBO-AlSC	2.50	0.0	60	10	24	0
CBO-TBABr	0.00	2.5	60	10	24	5
CBO-1	2.50	2.5	60	10	24	28
CBO-2	5.00	5.0	60	10	24	63
CBO-3	2.50	2.5	80	10	24	59
CBO-4	2.50	5.0	80	10	24	85
CBO-5	5.00	2.5	80	10	24	58
CBO-6	0.00	5.0	80	10	24	26
CBO-7	2.50	5.0	100	10	24	100
CBO-8	**1.25**	**5.0**	**100**	**10**	**24**	**100**
CBO-9	2.50	5.0	80	15	24	94
CBO-10	1.25	5.0	80	15	24	90
CBO-11	2.50	2.5	100	10	24	65
CBO-12	0.63	5.0	100	10	24	98
CBO-13	2.50	5.0	100	10	6	56
CBO-14	1.25	5.0	100	10	6	61
CBO-15	1.25	5.0	100	10	12	91
CBO-16	0.63	5.0	100	10	12	92
CMWO-1	2.50	2.5	80	10	24	63
CMWO-2	5.00	2.5	80	10	24	57
CMWO-3	2.50	5.0	80	10	24	93
CMWO-4	0.00	5.0	80	10	24	65
CMWO-5	2.50	5.0	100	10	24	100
CMWO-6	**1.25**	**5.0**	**100**	**10**	**24**	**100**
CMWO-7	2.50	5.0	80	15	24	99
CMWO-8	1.25	5.0	80	15	24	92
CMWO-9	2.50	5.0	100	10	6	71
CMWO-10	1.25	5.0	100	10	6	63
CMWO-11	1.25	5.0	100	10	12	97

*mol% per oxirane ring. The EBO has an average of 3.5 oxirane rings per triglyceride unit. The EMWO has an average of 4 oxirane rings per triglyceride unit.

The carbonation reactions using EMWO started at 80 °C, due to the results obtained using EBO. A screening process was also executed in a similar manner to the screening reactions performed for EBO. A conversion of 63% using 2.5 mol% of AlSC and 2.5 mol% of TBABr was obtained (CMWO-1). This result was close to CBO-3 (59%) which used the same reaction parameters. Moreover, increasing the TBABr load (5 mol%) raised the conversion to 93% (CMWO-3). Using only TBABr without AlSC achieved a conversion of 65% (CMWO-4), which was superior to CBO-6 (26%) under the same conditions. This difference and improvements in conversion can probably be related to the liquid nature of EMWO, which means TBABr solubilizes in EMWO more easily compared to EBO. Although BO melts above 45 °C,[14] it acts as a viscous liquid once in the liquid state. Furthermore, carbonation conversion reached 100% at 100 °C, using 2.5 mol% and 1.2 mol% of AlSC with TBABr, respectively (CMWO-5 and CMWO-6). Increasing the CO_2 pressure to 15 bar did not obtain a conversion of 100%. In this case, a loading of 2.5 mol% of AlSC under these conditions showed a conversion of 99% (CMWO-7). Results obtained after only 6 h also showed a lower conversion of 71% (CMWO-9). Thus, the time was increased to 12 h to obtain a conversion of 97% (CMWO-11). At the end of the screening experiments, the best result was that obtained for reaction CMWO-6. It was therefore affirmed that the best experimental conditions for the carbonatation reaction of EBO and EMWO are 100 °C with a CO_2 pressure of 10 bar for 24 h, using 1.2 mol% of AlSC and 5 mol% of TBABr. These conditions allowed 100% of the epoxide rings to be converted into carbonate rings.

On comparing these results to others in the literature, these results are comparable and better than those previously reported. Mazo and Rios in 2013 studied the carbonation reaction of epoxidized soybean oil (ESO) under conventional conditions with microwave heating (temperature = 140 °C under a continuous flow of CO_2), with TBABr (5.0 mol%) as a co-catalyst and water as a LA catalyst to active the epoxide ring. In this study the authors reached a conversion of 86.67% (under microwave conditions for 40 h) and 87.32% (using conventional means for 70 h).[18] In addition, Lee and Deng studied using a continuous flow of CO_2 in the carbonation reaction using TBABr (5.0 mol%) at 140 °C for ESO. However, they did not use any LA to improve the reaction. Consequently, the reaction took 72 h to reach 100% conversion.[19] Tamami *et al.* obtained a conversion of 100% for ESO after 70 h, also using a continuous flow of CO_2 and a load of 5 mol% of TBABr at 110 ºC. [20] Furthermore, Parzuchowski *et al.* studied ESO carbonation using a high temperature (130 ºC) and CO_2 pressure (60 bar) to achieve a conversion of 98.3% after 120 h, using 18-crown-6 as catalyst and potassium iodide (KI) as a co-catalyst. [21] A carbonation conversion of 100% after 48 h was reached using ESO and epoxidized linseed oil (ELO) at a pressure of 10 bar and a higher temperature of 140 °C using TBABr without a LA, which is double the reaction time of this study.[22] Zhang *et al*. described a conversion of 100% in the carbonation of epoxidized cotton oil (ECO) after 24 h using only TBABr. This conversion however required the reactor to be heated to 140 °C and a higher pressure (30 bar).[23] Dong *et al*. obtained a conversion of 100% in 12 h for ESO at 120 °C and 50 bar, using a catalytic system of $MgCl_2$/TBABr.[24] Liu *et al.* used a catalyst system of TBAI/L-ascorbic acid to obtain a conversion of 82% (temperature = 80 °C; pressure = 35 bar; and time = 48 h).[17] Other works in the literature describe the use of much higher pressures (103 bar) at 100 °C to obtain a conversion of 100% for carbonated soybean oil in 40 h.[25] The fastest time in an ESO carbonation reaction was described by Poussard *et al.*, who used only TBABr (2.65 mol%) in supercritical CO_2 conditions (T=120 °C and P=100 bar) to reach 100% conversion in 9 h.[26] Overall, it is possible to conclude that AlSC acts as an excellent catalyst to improve the carbonation reaction of epoxidized vegetable oils, when compared to other experimental parameters reported in the literature.

Mid-Infrared Spectroscopy (MIR), ^{1}H-NMR, and ESI-Mass spectrometry analyses of carbonated oils.

MIR spectra for EBO and different reaction mixtures after the carbonation process were analysed and compared. The products obtained from the reactions CBO-TBABr (where conversion was 5%), CBO-1 (28%), CBO-5 (58%), CBO-4 (85%) and CBO-8 (100%) can be seen, and are compared to the EBO spectrum, in Figure 2a. The carbonation reaction of EBO turns epoxide rings into five-membered cyclic carbonates, therefore a new carbonyl group stretching band (C=O) appears at 1803 cm^{-1} (highlighted in blue). As expected, CBO-8 has a more intense band than CBO-TBABr. The band at 1741 cm^{-1} was related to C=O stretching of the glycerol-fatty esters. In addition, the band at 1043 cm^{-1} (highlighted in green) was attributed to -O-C=O-O- stretching of the five-membered ring.[23] Finally, a mid-intensity band at 775 cm^{-1} (highlighted in red) was related to C-H bending in the α-position of the carbonate group.[26]

The ^{1}H-NMR spectrum for EBO shows a singlet at 2.85 ppm, a multiplet at 2.94 ppm and another multiplet at 3.06 ppm, related to hydrogens in the epoxide rings (highlighted in blue, Figure 2b). After the carbonation reaction these signals vanish due to the reaction with CO_2 forming five-membered cyclic carbonate groups. Due to the high negative electron density in the cyclic carbonate structure, the hydrogen signal appears at a higher ppm, between the hydrogens of the glycerol backbone at 4.2 ppm and 5.5 ppm. Therefore, 4 new signals can be seen (highlighted in red), a multiplet at 4.47 ppm, a doublet at 4.59 ppm, a triplet at 4.73 ppm and another multiplet at 4.87 ppm. Consequently, CBO-8 which has a conversion of 100%, does not present a signal related to the epoxide ring, with the spectrum exhibiting four well-defined signals of the hydrogens in the cyclic carbonate groups. In addition, all ^{1}H-NMR spectra for CBO and CMWO can be seen in the supporting information (Figure S4 to Figure S32 in the Supporting Information).

The product formed from the CBO-8 reaction (which achieved a conversion of 100%) was also analyzed by ESI-Mass Spectrometry, as shown in Figure 2c. It is important to emphasize that signals contain an additional 22.9897 *m/z* due to the presence of sodium (Na^+) ions. The ion at *m/z* 1087.7271 is associated with a CBO with three cyclic carbonates (1064.7374 Da); whilst, *m/z* 1129.6651, m/z 1043.7374 and *m/z* 999.7488 are related to CBO structures with four cyclic carbonates (1106.6754 Da), two cyclic carbonates (1020.7227 Da) and one cyclic carbonate (976.7174 Da), respectively. This was expected as the vegetable oil is a mixture of different triacylglycerols with three fatty acids, which can be unsaturated or saturated. Therefore, the carbonated structure depends on the initial unsaturation quantity. Furthermore, the difference of 28 mass units (green arrow in Figure 2c) is associated with two methylene groups (CH_2CH_2),[26] probably due to fatty acid chain diversity. This can be expected, as the starting BO material contains palmitic acid (C16:0), oleic acid (C18:1), linoleic acid (C18:2), linolenic acid (C18:3), eicosenoic acid (C20:1) as well as erusic acid (C22:1).[14] Lastly, the yellow arrow in Figure 2c shows a fragment of 14 Da (CH_2) which can be related to fatty acid diversity.

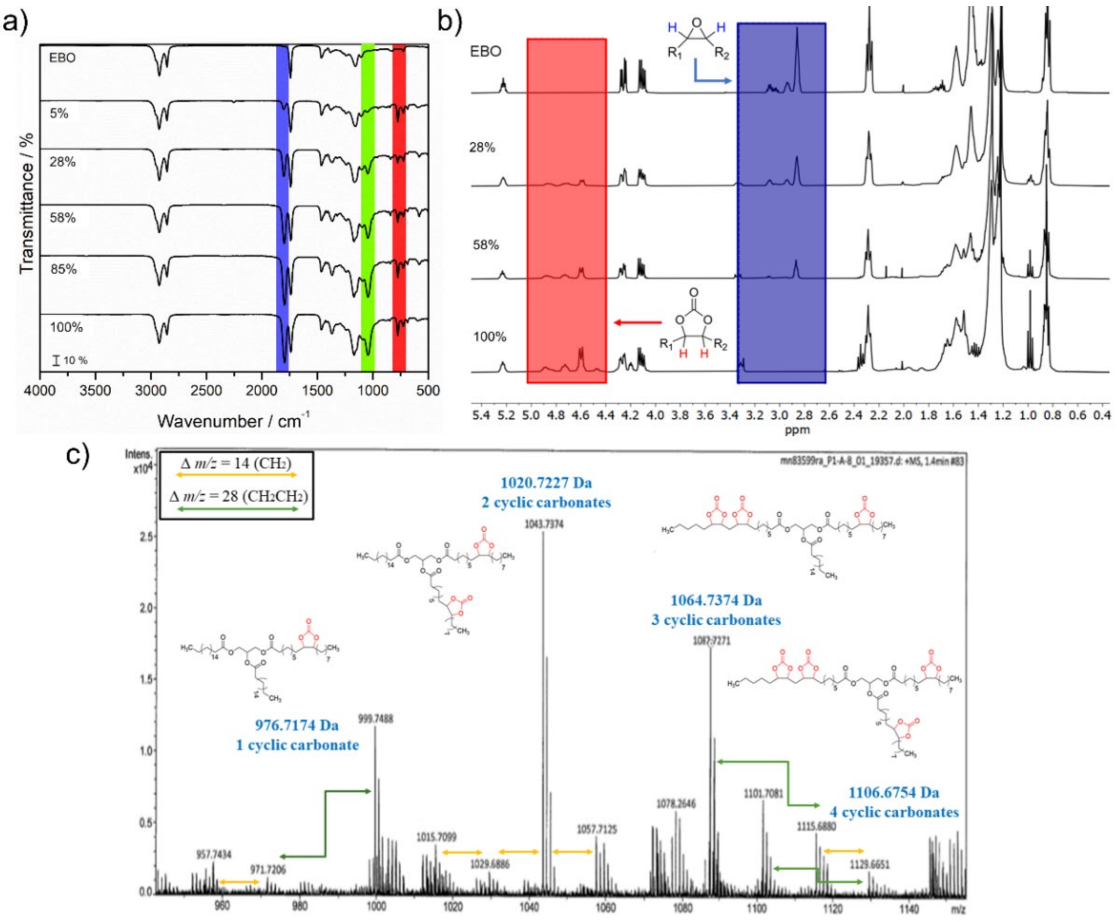

Figure 2. (a) MIR spectra of EBO, CBO-TBABr, CBO-1, CBO-5, CBO-4, and CBO-8; (b) ^{1}H-NMR spectra of EBO, CBO-1, CBO-5, and CBO-8; and (c) ESI-Mass spectrum of CBO-8 after purification.

Synthesis and MIR characterization of CMWO and CBO polyurethanes.

The polymers were synthesized by reacting CMWO or CBO with different amines in an equimolar ratio. The amines selected are classed as sustainable, which is ideal to produce sustainable bio-based polymers. HDA is derivable from biomass and LYS is an inexpensive amino acid, which can be produced on a large scale via a fermentation process.[27] Although the MBCA is not a bio-based derivative, it is relatively inexpensive and has already been used as a cross-linker in other polymer syntheses.[28,29]

The amine reacts with the carbonate by a nucleophilic acyl substitution reaction to form a urethane linkage and leaves a hydroxyl group attached to the triglyceride structure. This type of reaction occurs easily and no catalyst is needed. However, the amine can also react with the glyceride part,[17,24,30] releasing glycerol as a by-product and forming a non-desire linkage, which can spoil the cross-linking structure. This therefore means that the reaction often requires more time to reach an adequately polymerized material. The occurrence of both reactions was confirmed by MIR spectroscopy. Figure 3a and 3b display the MIR spectra (at different times) for CMWO and CBO polymers with HAD as a cross-linker, respectively. The peak at 1809 cm^{-1} is related to C=O bond stretches in the cyclic carbonate (highlighted in blue), and the band at 1745 cm^{-1} (marked with an orange dashed line) is related to the C=O of the glyceride structure. Both bands have high intensity at the beginning of the reaction (i.e. at 0 h) and are then consumed during the reaction progress. New bands (highlighted in purple) were formed during the reaction. The first is related to C=O stretches of urethane groups at 1739 cm^{-1}. Two new bands appear at 1641 cm^{-1} and at 1553 cm^{-1} and are associated with the N-H bending vibrations of primary and secondary amides, respectively.[24] The band at 3317 cm^{-1} could be associated with O-H stretches of the alcohol group attached at the fatty acid chain, or the presence of glycerol released during the reaction. The MIR spectra for CMWO and CBO polymers with LYS and MBCA are shown in the supporting information (Figures S33 and S34).

Although the carbonate conversion was not complete after 72 h, the polymer presented a solid form after this time, had a dark brown color appearance, and rubbery characteristics. Figure 3c and 3d show the conversion of carbonate and glyceride (a non-desired side-reaction), respectively. Each amine compound (cross-linker) showed different carbonate conversions. The CMWO-HDA and CMWO-MBCA reached a carbonated conversion of 81%, while CBO-HDA and CBO-MBCA both presented a carbonated conversion of 72%. The CMWO-LYS and CBO-LYS achieved the same conversion of 45% after 120 h. This lower and slower conversion result can be justified by the presence of a carboxylic acid in the lysine structure, which can consequently protonate an amine group and thus give an ammonium ion and carboxylate (i.e. produce a zwitterion). Therefore, the ammonium ion is not able to attack the cyclic carbonate group. The HAD and MBCA cross-linkers attacked the glyceride group more efficiently, both showing conversions above 50%. However, LYS is more selective towards carbonate groups, giving a low glyceride conversion (conversions of 13% and 25% were obtained for CMWO-LYS and CBO-LYS, respectively).

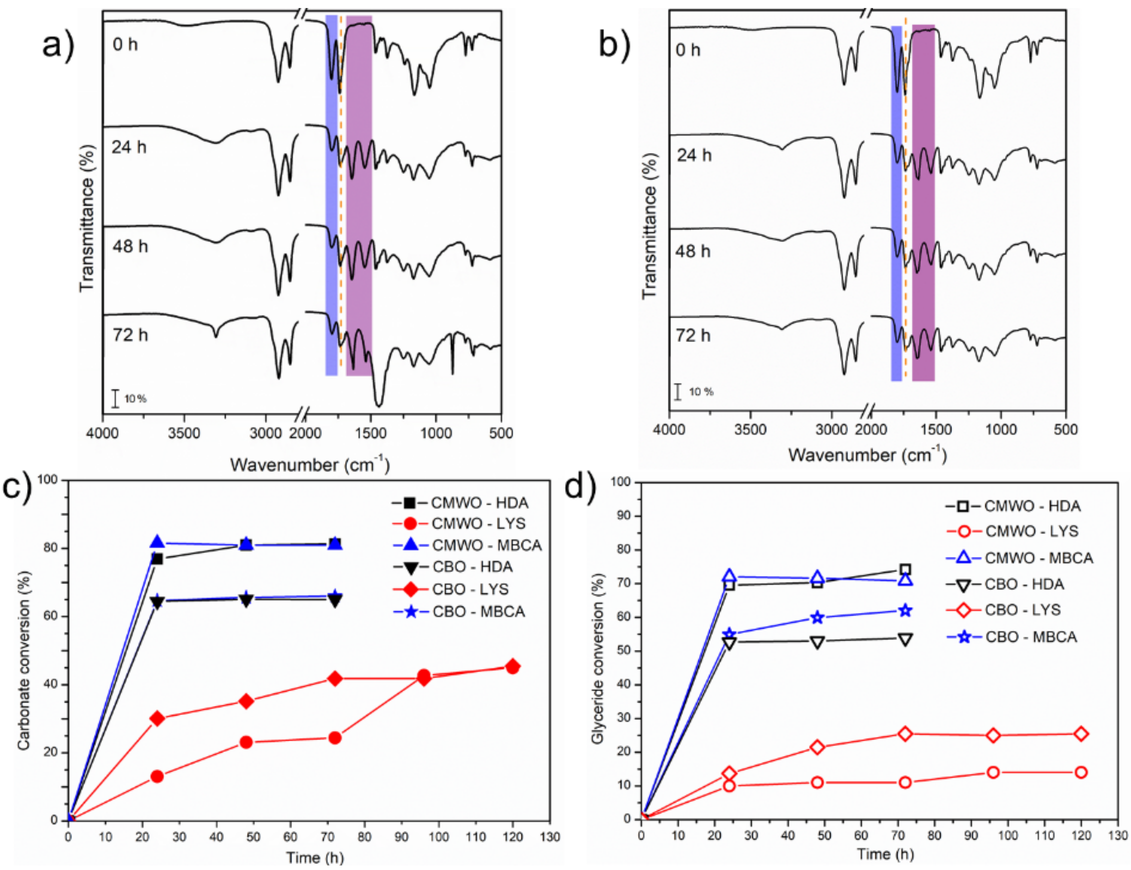

Figure 3. a) MIR spectra for polymers at different times using CMWO as monomer and HDA as cross-linker; b) MIR spectra for polymers at different times using CBO as monomer and HDA as cross-linker; c) conversion of cyclic carbonate over time; and d) conversion of glyceride over time.

Thermal and mechanical properties, reshaping property, cross-linking density, and gel content

The TG and DTG curves for CMWO-HDA (Figure 4a) indicate that the sample is thermally stable up to 230 °C and decomposes in two mass loss steps. The first step (231-480 °C) appears as a simple process in the TG results. However, in DTG analysis, multiple decomposition steps are observed other this temperature range, indicating a complex process that has consecutive and overlapped decompositions. This corresponds to polymeric matrix degradation and fatty chain degradation.[31,32] The second step of mass loss started at 480 °C and finished at 634 °C, and is associated with the degradation and oxidation of carbonaceous material formed in the first step. Moreover, each step of mass loss is linked to an exothermic peak in the DTA curve. The TG, DTG, and DTA curves for CBO-HDA (Figure 4b) have a similar thermal profile to CMWO-HDA, and the sample presents thermal stability up to 231 °C.

The CMWO-LYS presents thermal stability up to 204 °C as displayed by the TG and DTG curves (Figure 4a). The first step of mass loss is related to residual lysine degradation and a decarboxylation process,[33] which justifies its lower mass variation (3.1%). The second step of mass loss (at 262-475 °C) is associated with cross-linker and fatty acid chain degradation, while the third mass loss step is related to carbonaceous oxidation and degradation. The CBO-LYS presents a similar thermal profile as shown by TG, DTG, and DTA curves (Figure 4b), with thermal stability up to 204 °C.

The TG curve for CMWO-MBCA shows that the sample is thermally stable up to 249 °C, and then decomposes in two mass loss steps, though the first step is a complex process as seen in the DTG curve. The first step of mass loss begins at 249 °C and finishes at 505 °C, and is associated with polymeric matrix degradation. As previously discussed for the other samples, the second mass loss step (505-634 °C) is related to the degradation of carbonaceous matter. As expected, the TG/DTG-DTA curves for the CBO-MBCA (Figure 4b) have a similar thermal profile to CMWO-MBCA, and the same thermal stability (249 °C).

Table 2 displays thermal information relating to each polymer. All polymers presented thermal stability above 200 °C, illustrating a relatively high thermal stability. The highest stable temperature was achieved using MBCA as a cross-linker (249 °C).

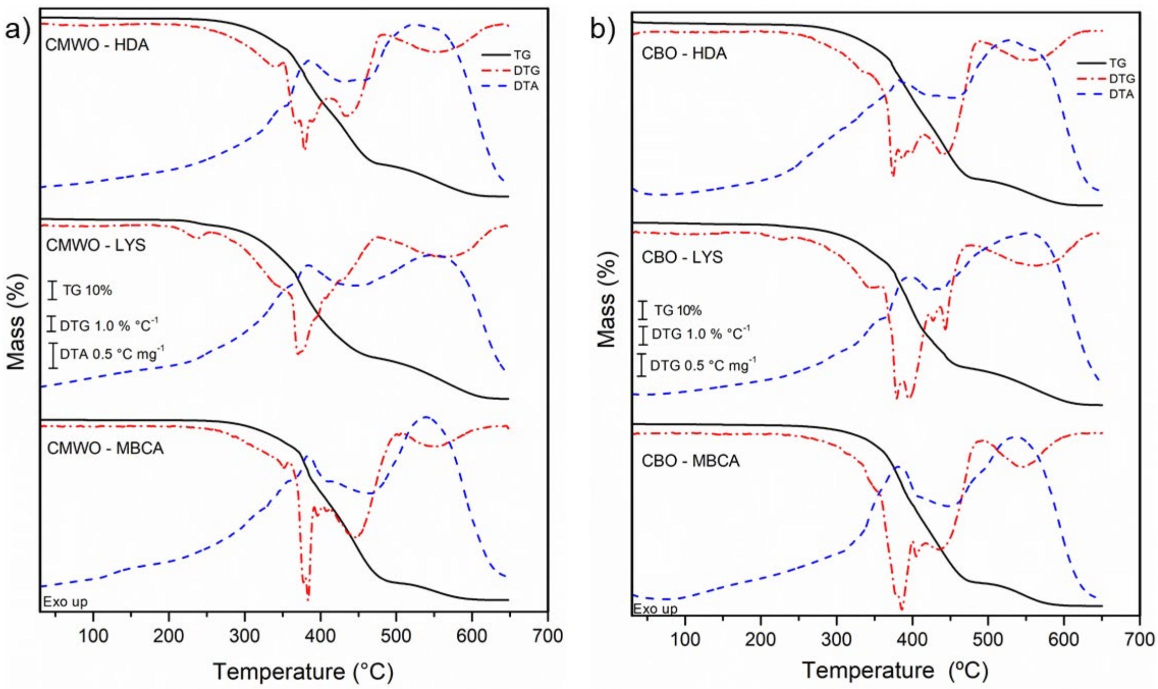

Figure 4. a) TG/DTG-DTA curves for CMWO polymers; and b) TG/DTG-DTA curves for CBO polymers.

Table 2. Summary of the polymers mass loss events (Δm/%). The temperature range in which each event occurred (θ °C) and the temperature peak (T_P/°C) are also given.

Polymers			1st Step	2nd Step	3rd Step
CMWO	HDA	θ °C	231-480	480-634	-
		Δm/%	79.5	20.5	-
		T_P/°C	385↑	523↑	-
	LYS	θ °C	204-262	262-475	475-640
		Δm/%	3.1	72.4	24.5
		T_P/°C	-	384↑	547↑
	MBCA	θ °C	249-505.3	505-634	-
		Δm/%	88.9	11.1	-
		T_P/°C	382↑	539↑	-
CBO	HDA	θ °C	231-489	489-643	-
		Δm/%	84.5	15.5	-
		T_P/°C	381↑	527↑	-
	LYS	θ °C	204-263	263-475	475-662
		Δm/%	2.1	76.5	21.4
		T_P/°C	-	397↑	552↑
	MBCA	θ °C	249-490	490-620	-
		Δm/%	85.9	14.1	-
		T_P/°C	382↑	537↑	-

↑=Exothermic peak

The DSC curves for each polymer (Figure 5a and 5b) present two thermal events. The first one is associated with a glass transition temperature (T_g). At temperatures below T_g, the polymer is in its vitreous state and presents hardness and brittle features.[31] Above

T_g, the polymer reaches its rubbery state, exhibiting malleability and soft features. The second event is related to the topology-freezing transition temperature (T_v). Above T_v, the polymer is more malleable and rapid bond exchange can be achieved, so the material changes from a viscoelastic solid to a viscoelastic liquid. This feature is common in vitrimers, which are polymers with a thermosetting configuration. These polymers can also be remolded as thermoplastics or present a welding property (i.e. act as self-healing polymers).[34,35] Both events are reversible, as confirmed by performing a second heating cycle (as shown in Figure S35 to S40 in the Supporting Information). The T_g and T_v values from the DSC curves for each polymer are summarized in Table 3.

DMA was used to confirm the T_g results observed during DSC analyses. The DMA curves (Figure 5c) of CMWO-HDA, CMWO-LYS, CBO-HDA, and CBO-LYS show the storage modulus (E') and the tan-δ values obtained. The peak temperature of the tan-δ curve represents the T_g temperatures and are close to those found in the DSC analysis. The DMA curves for CMWO-MBCA and CBO-MBCA are not seen, because of their higher vitreous properties. Below the T_g temperature, these samples turn into a highly brittle material. Therefore, their analyses were not successful, as the samples fractured at -20 °C. The T_v temperatures are not observed in the DMA curves, due to their lower intensity compared to their T_g values. The tan-δ temperatures are shown in Table 3.

The stress-strain curves can be seen in Figure 5d. The CMWO-HDA and CBO-HDA reached high strains of 61% and 44%, respectively. This elastic property can be associated with the cross-linker HDA, which is linear and has six carbons, therefore providing more bond movements.[36] CMWO-HDA and CBO-HDA achieved a good stress resistance before breaking at 1.6 MPa and 1.5 MPa, respectively. The MBCA polymers had a lower strain but similar stress properties to the HDA polymers. The LYS polymers presented the lowest strain properties, which means they had a harder and more fragile structure under stress, despite LYS containing a linear structure with five carbons. This can be attributed to hydrogen bonds formed between the amines and the carboxylic acid. The CMWO-LYS and CBO-LYS samples have similar stress properties to HDA and MBCA polymers. Each property regarding mechanical analysis can be seen in Table 3.

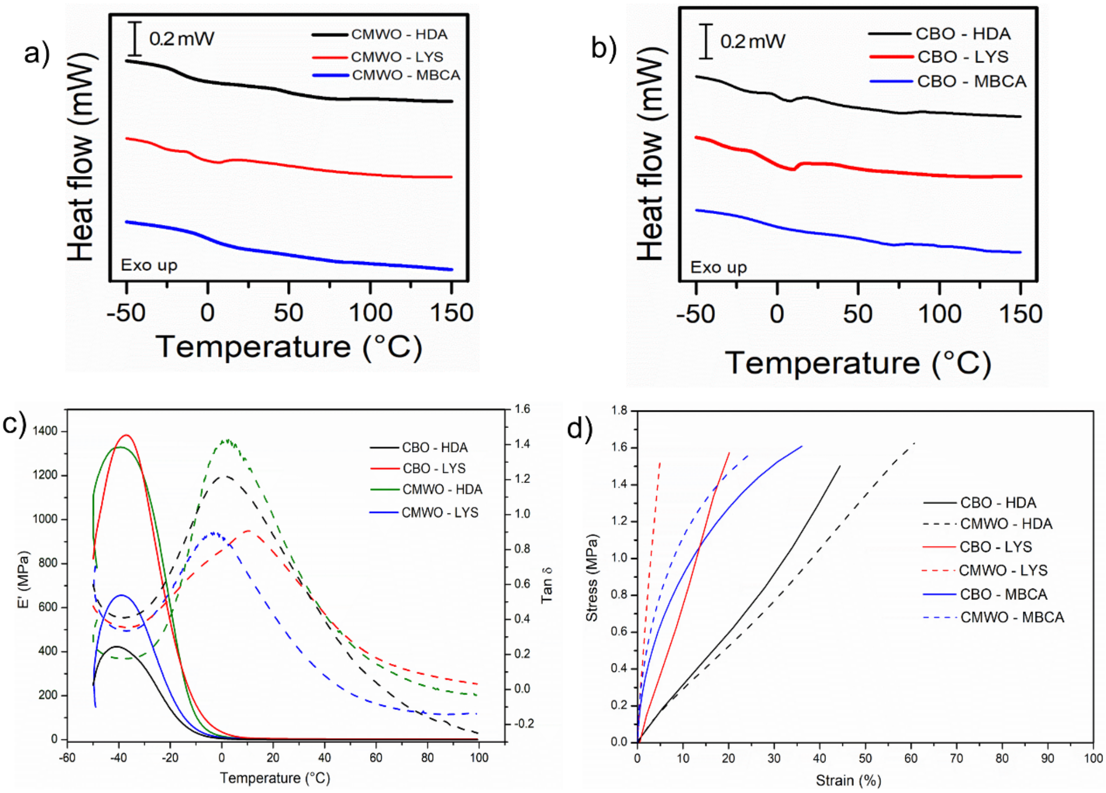

Figure 5. a) DSC curves for CMWO polymers; b) DSC curves for CBO polymers; c) DMA results for the CMWO and CBO polymers showing storage modulus – E' (dashed line) and tan-δ (solid line); and d) stress-strain experiment results for each polymer.

Table 3. Thermal, mechanical and cross-linking properties of the polymers.

	CMWO			CBO		
	HDA	**LYS**	**MBCA**	**HDA**	**LYS**	**MBCA**
T_g – DSC (°C)	-11.5	9.4	-0.8	0.3	12.2	-0.8
T_v – DSC (°C)	46.6	46.9	50.8	60.4	52.5	62.7
Tan-δ (°C)	1.7	-3.5	-	0.8	10.2	-
Stress (MPa)	1.6	1.5	1.6	1.5	1.6	1.6
Strain (%)	61.3	5.0	24.3	44.6	20.3	36.4
Gel content (%)	62.1	65.2	47.7	45.3	52.9	38.4
Cross-linking Density (mol m^{-3})	91.8	159.1	-	24.3	148.7	-

The welding process of vitrimers derived from bio-based polymers is extensively studied nowadays.[34,35] For most polymers, the welding process needs temperatures above 130 °C, a high pressure (70-100 bar), and an excessive time period (> 2 h). Therefore, we have developed a new welding process using red light (660 nm) in a Teflon® cast. These polymers can absorb the red light, which results in the polymer heating up and quickly raising the desired high temperature. Figure 6a illustrates the process of preparing the CMWO-HDA sample, which was cut into pieces, and then added to a circular cast prior to irradiation. The polymer pieces were then irradiated by a red light (660 nm) for 2 minutes, reaching a temperature of 122 °C. Thereafter, the light was turned off and the polymer was pressed with an aluminum support. After cooling to room temperature, the polymer can be removed from the casting mold, forming a new shape and is totally welded. This is easier and faster than other methods reported in the literature.[17,24,30,37,38] The temperature reached under the red light after 2 minutes is sufficient to surpass the T_v of each polymer. Therefore, bond exchange can be achieved by a transcarbomoylation reaction between the urethane and alcohol groups linked on the polymer structure.[39] The proposed scheme for this bond exchange is exhibited in Figure 6b.

The gel content parameter (Figure 6c) gives information about the polymer curing and its cross-linking network. None of these polymers achieved a 100% gel content, which would indicate a complete cure and a fully cross-linked structure.[30] This can be associated with the side reaction involving glyceride groups, which releases glycerol and spoils the cross-linking process. This is consistent with the MIR spectroscopy analyses and the conversion results discussed earlier. CMWO polymers showed a better gel content than CBO, as they have four carbonate groups which favors the cross-linking process.

The cross-linking density (Figure 6c) also provides information about how well a polymer is cross-linked. This information is acquired from the DMA curves and Eq. 2. The result obtained is in accordance with the MIR spectroscopy analyses. Therefore, the best polymers obtained were those using LYS as a cross-linker, which provides fewer side reactions with glyceride. The cross-linking densities for CMWO-MBCA and CBO-MBCA could not be obtained due to experimental difficulty in DMA analysis (as mentioned previously).

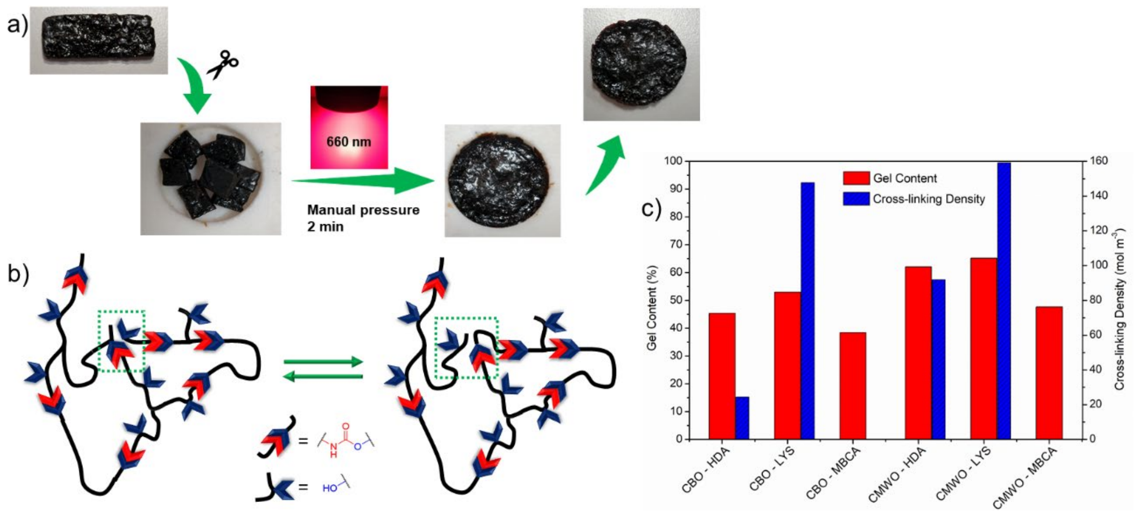

Figure 6. a) Reshaping of CMWO-HDA under red light (660 nm); b) general scheme for the self-healing property by OH exchange; and c) gel content and cross-link density results.

CONCLUSIONS

Carbonation reactions of EBO and EMWO were performed, resulting in 100% conversion of epoxide rings into five-membered cyclic carbonates using CO_2 gas as the carbon source. The process occurred using TBABr and an aluminum(salen) complex (AlSC) as the catalytic system. A screening method was executed resulting in the best synthetic parameters, which determined as temperature = 100 °C, pressure of CO_2 = 10 bar, time = 24 h, TBABr concentration = 5.0 mol%, and AlSC concentration = 1.2 mol% (with respect to epoxide). The method used in this study presents advantages compared to previously reported literature methods. This study illustrates that AlSC is a promising catalyst for the carbonation of vegetable oils, and thus can be used to carbonate other vegetable oils, such as soybean, linseed and sunflower oil etc. Furthermore, macaw oil and baru oil are good substitutes for soybean oil, and could be further studied for other polymer reactions and syntheses. Spectroscopic analysis (MIR and ^{1}H-NMR) and ESI-mass spectrometry were fundamental to determine the conversion of each carbonation reaction, and confirmed the functional and structural modification of the Baru and Macaw oil. The ESI-mass spectra showed that final product - CBO can contain structures with one, two, three or four cyclic carbonates. CMWO and CBO underwent polymerization on treatment with diamines and cross-linking occurred through the carbonate groups, though some side reactions were observed and confirmed by MIR spectroscopy. LYS exhibited a more selective reaction towards the carbonate groups, thus providing a better cross-linked structure as confirmed by gel content results and cross-linking density analysis (DMA). All the polymers presented good thermal stability, withstanding temperatures above 200 °C. DSC analyses indicated events related to the glass transition temperature (T_g) and the topology-freezing transition temperature (T_v), permitting an exchange of bonds and hence a welding process. The welding process is achieved via a novel, greener, faster, and easier method (compared to traditional means) by using red light (660 nm).

ACKNOWLEDGMENTS

The authors wish to thank São Paulo Research Foundation - FAPESP (grant 2019/11493-4, 2021/14879-0, and 2021/02152-9), CAPES (grants 024/2012 and 011/2009 Pro-equipment), and CNPq (grant 303247/2021-5) for financial support.

REFERENCES

1. L. Guo, K. J. Lamb, M. North, *Green Chem*. **2021**, *23*, 77-118.

2. P. P. Pescarmona, *Curr. Opin. Green Sust. Chem*. **2021**, *29*, 100457.

3. M. North, *ChemSusChem*. **2019**, *12*, 1763-1765.

4. M. North, *What is CO_2? Thermodynamics, Basic Reactions and Physical Chemistry. In: CARBON Dioxide Utilisation: Closing the Carbon Cycle*. Elsevier, **2015**.

5. M. North, R. Pasquale, R. C. Young, *Green Chem*. **2010**, *12*, 1514-1539.

6. Y. Zhu, C. Romain, C. K. Williams, *Nature*. **2016**, *540*, 354-362.

7. A. Gomez-Lopez, S. Panchireddy, B. Grignard, I. Calvo, C. Jerome, C. Detrembleur, H. Sardon, *ACS Sust. Chem. Eng*. **2021**, *9*, 9541-9562.

8. European Bioplastics. https://www.european-bioplastics.org/market/, 2022 (accessed 09 September 2022).

9. R. T. Alarcon, K. J. Lamb, G. Bannach, M. North, *ChemSusChem*, **2021**, *14*, 169-188.

10. X. Wu, C. Chen, Z. Guo, M. North, A.C. Whitwood, *ACS Catalyst*. **2019**, *9*, 1895-1906.

11. W. Clegg, R. W. Harrington, M. North, R. Pasquale, *Chem. Euro. J.* **2010**, *16*, 6828-6843.

12. J.W. Comerford, I.D.V. Ingram, M. North, X. Wu, *Green Chem*. **2015**, *17*, 1966-1987.

13. ASTM D5554-15, *Standard test method for determination of the iodine value of fats and oils*, **2015**.

14. R. T. Alarcon, C. Gaglieri, K. J. Lamb, M. North, G. Bannach, *Ind. Crops Prod*. **2020**, *154*, 112585.

15. ASTM DAS1652-11, 2019. *Standard test method for epoxy content of epoxy resins*.

16. X. Liu, X. Yang, S. Wang, S. Wang, Z. Wang, S. Liu, X. Xu, H. Liu, Z. Song, *ACS Sustain. Chem. Eng*. **2021**, *9*, 4175–4184.

17. P. Mazo, L. Rios, *J. Am. Oil Chem. Soc*. **2013**, *90*, 725-730.

18. A. Lee, Y. Deng, *Euro. Polym. J.* **2015**, *63*, 67-73.

19. B. Tamami, S. Sohn, G.L. Wilkes, *J. Appl. Polym. Sci*. **2004**, *92*, 883-891.

20. P. Parzuchowski, M. Jurczyk-Kowalska, J. Ryszkowska, G. Rokicki, *J. Appl. Polym, Sci*. **2006**, *102*, 2904-2914.

21. B. Moritz, R. Mülhaupt, *Green Chem*. **2012**, *14*, 483-489.

22. L. Zhang, Y. Luo, Z. Huo, Z. He, W. Eli, *J. Am. Oil Chem. Soc*. **2014**, *91*, 143-150.

23. J. Dong, B. Liu, H. Ding, J. Shi, N. Liu, B. Dai, I. Kim, *Polym. Chem*. **2020**, *11*, 7524-7532

24. K. Doll, S. Erhan, *Green Chem*. **2005**, *7*, 849-854.

25. L. Poussard, J. Mariage, B. Grignard, C. Detrembleur, C. Jérôme, C. Calberg, B. Heinrichs, J. De Winter, P. Gerbaux, J. M. Raquez, L. Bonnaud, P. Dubois. *Macromol*. **2016**, *49*, 2162-2171.

26. J. H. Clark, T. J. Farmer, I. D. V. Ingram, Y. Lie, M. North. *Euro. J. Org. Chem*. **2018**, *31*, 4265-4271.

27. N. Liang, E. Fujiwara, M. Nara, R. Ishige, S. Ando, *ACS Appl. Polym. Mater*. **2021**, *3*, 3911-3921.

28. G. Liu, G. Wu, S. Huo, C. Jin, Z. Kong, *Prog. Org. Coat*. **2017**, *112*, 169-175.

29. X. Yang, C. Ren, X. Liu, P. Sun, X. Xu, H. Liu, M. Shen, S. Shang, Z, Mater. *Chem. Front*. **2021**, *5*, 6160-6170.

30. R. T. Alarcon, C. Gaglieri, O. A. Souza, D. Rinaldo, G. Bannach, *J. Polym. Envir*. **2020**, *28*, 1265-1278.

31. C. Gaglieri, R. T. Alarcon, A. Moura, R. Magri, L. C. Silva-Filho G. Bannach, *J. Braz. Chem. Soc*. **2021**, *32*, 2120-2131.

32. T. S. Martins, J. R. Matos, G. Vicentini, P.C. Isolani, *J. Therm. Anal. Calorim*. **2005**, *82*, 77-82.

33. J. Zheng, Z. M. Png, S. H. Ng, G. X. Tham, E. Ye, S. S. Goh, X. J. Loh, Z. Li, *Mater. Today*. **2021**, *51*, 586-625.

34. F. Hajiali, S. Tajbakhsh, M. Maric, *Polym*. **2021**, *212*, 123126.

35. C. Ding, P. S. Shuttleworth, S. Makin, J. H. Clark, A. S. Matharu, *Green Chem*. **2015**, *17*, 4000-4008.

36. X. Chen, L. Li, K. Jin, J.M. Torkelson, *Polym. Chem*. **2017**, *8*, 6349-6355.

37. S. Hu, X. Chen, J. M. Torkelson, *ACS Sust. Chem. Eng*. **2019**, *7*, 10025-10034.

38. M. A. Lucherelli, A. Duval, L. Averous, *Prog. Polym. Sci*. **2022**, *127*, 101515.